

Supporting Information for the Paper

Bent Keto Form of Curcumin, Preferential Stabilization of Enol by Piperine, and Isomers of Curcumin \cap Cyclodextrin Complexes: Insights from Ion Mobility Mass Spectrometry

Abhijit Nag[†], Papri Chakraborty[†], Ganapati Natarajan[†], Ananya Baksi[†], Sathish Kumar Mudedla[‡], Venkatesan Subramanian[‡] and Thalappil Pradeep^{*†}

[†]DST Unit of Nanoscience and Thematic Unit of Excellence, Department of Chemistry, Indian Institute of Technology Madras, Chennai-600036, India

*Email: pradeep@iitm.ac.in

[‡]Chemical Laboratory, CSIR-Central Leather Research Institute, Adyar, Chennai 600020, India

Table of contents

Name	Description	Page no.
	Experimental and computational details	S4-S7
Figure S1	Fragmentation of keto-enol forms of curcumin	S8
Figure S2	Schematic representation of cis keto-enol forms of curcumin	S9
Figure S3	DFT optimized EDP (CE1-H) ⁻ structure	S9
Figure S4	Bending angles of keto forms	S10

Table S1	Experimental and theoretical CCS values	S10
Figure S5	Solvent dependent study of keto-enol isomers	S11
Figure S6	Plot of the natural logarithm of enol/keto peak intensity ratios against the desolvation gas temperature	S12
Figure S7	Plot of the natural logarithm of enol/keto peak intensity ratios against the different cone voltages	S13
Figure S8	Cone voltage dependent fragmentation study	S14
Figure S9	UPLC separation of keto-enol forms of curcumin	S15
Figure S10	ESI MS of the supramolecular complex of curcumin-piperine	S16
Figure S11	DFT optimized structures of (CE1-H) ⁻ -piperine interactions	S17
Figure S12	DFT optimized structures of (CE2-H) ⁻ -piperine interactions	S18
Figure S13	DFT optimized structures of (CK1-H) ⁻ -piperine interactions	S19
Figure S14	DFT optimized structures of (CK2-H) ⁻ -piperine interactions	S20
Table S2	Relative energies of the (curcumin-H) ⁻ -piperine complexes	S21
Table S3	Most stable curcumin-piperine complexes with their interaction energies	S21
Table S4	Most stable (curcumin-H) ⁻ -piperine complexes with their interaction energies	S22

Figure S15	DFT optimized lowest energy structures of CE1-piperine, CE2-piperine, CK1-piperine and CK2-piperine, respectively	S22
Figure S16	Drift time profile of curcumin- β -cyclodextrin (1:2) inclusion complex	S23
Figure S17	Drift time profile of curcumin- α -cyclodextrin (1:1) inclusion complex	S24
Figure S18	CE1 and CK1 docked β -cyclodextrin structures, respectively with binding energies	S25
Figure S19	Docking of β -cyclodextrin-CE1 and β -cyclodextrin-CK1, respectively with second β -cyclodextrin	S25
Figure S20	CE1 docked β -cyclodextrin dimer structures at different distances of cyclodextrin dimers	S26
Figure S21	CK1 docked β -cyclodextrin dimer structure with different angles of cyclodextrin dimers	S26
Table S5	CE1-docked β -cyclodextrin dimers with binding energies and CCS values	S27
Table S6	CK1-docked β -cyclodextrin dimers with binding energies and CCS values	S27

Experimental methods

Chemicals

Curcumin (C₂₁H₂₀O₆, 94% pure), piperine (C₁₇H₁₉NO₃, 97% pure), α -cyclodextrin (C₃₆H₆₀O₃₀, 98% pure), and β - cyclodextrin (C₄₂H₇₀O₃₅, 97%) were obtained from Sigma-Aldrich. Methanol (99.9 % pure), Hexane (97% pure), DMSO (99.9% pure) and milli Q water were used throughout the experiment.

Instrumentation

All mass spectrometric measurements were conducted using a Waters Synapt G2Si High Definition Mass Spectrometer equipped with electrospray ionization (ESI) and ion mobility (IM) separation. All the samples were analyzed in negative ESI mode. The instrument was calibrated using sodium formate (m/z 20–1500) as a calibrant for the low mass range. For IMS measurements, the ions of interest were selected by a quadrupole mass filter and passed through the IMS cell for isomer separation where nitrogen was used as a buffer gas. Typical experimental parameters were: desolvation gas temperature, for temperature dependent, study it was varied from 40 to 600 °C ; capillary voltage, 3 kV; sample cone, 0 V; source offset, 0 V; trap collision energy, 2 V; trap gas flow, 2 mL/min; helium cell gas flow, 180 mL/min; IMS gas flow, 80 mL/min; trap DC bias, 40 V; IMS wave height, 40 V and IMS wave velocity, 750 m/s. The collision voltage in the transfer cell was raised until fragmentations were seen properly (4-60 V). The concentration of the sample was 0.05 mM and it was infused at a flow rate of 10 μ L/min.

Parameters for cyclodextrin-curcumin inclusion complexes: Capillary voltage, 3 kV; sample cone, 20 V; source offset, 20 V; trap collision energy, 2 V; trap gas flow, 2 mL/min; helium cell gas flow, 180 mL/min; IMS gas flow, 80 mL/min; trap DC bias, 40 V; IMS wave height, 40 V; IMS wave velocity, 400 m/s.

We used the recent literature on negative ion mode traveling wave ion mobility mass spectrometry calibrations.¹ Polyalanine was used as a calibrant. We compared the CCS values of Leucine enkephalin with a reported paper.¹ Then we carried out the experiments.

UPLC Separation Method

Standard curcumin solutions (0.05 mM in methanol) were prepared. The UPLC instrument is ACQUITY from Waters. An ACQUITY UPLC BEH C18 1.7 μ column was kept at 40 °C. The

mobile phase was water/acetonitrile (50/50). The flow rate of the mobile phase was set at 0.5 mL/min. Mass spectrometry data were collected using a Waters Synapt G2Si High Definition Mass Spectrometer equipped with electrospray ionization (ESI) in the negative ion mode. The capillary voltage was 3.0 kV for negative ion detection. MS/MS fragmentation spectra of curcumin were acquired with the precursor ion, m/z 367.

ESI MS for curcumin-piperine interactions

The ESI MS for curcumin piperine interactions has been performed in ethanol.

Computational methods

Initial geometries of the curcumin was taken from the PDB files (enol), cif files (enol)²⁻⁵ in the literature, and also built from their structural formulae using Avogadro software.⁶ Since only the enol form has been crystallized, we built the keto structure by modifying the enol group by moving the H atom and the initial keto geometry was supported by a co-crystal structure.⁶ First, we carried out a conformational isomer search on the enol and keto forms of curcumin using a genetic algorithm and weighted rotor searches using Avogadro. The parameters of the genetic algorithm were, Children=10, Mutability=10, and Convergence=50 Scoring method=Energy. We used an MMFF94 force field. All the structures were modeled by utilizing Avogadro software packages⁶ and the visualizations presented were created using Visual Molecular Dynamics (VMD) software.⁷ The crystal structures of alpha-CD⁸ and beta-CD⁹ were taken from PDB files. The enol form was unchanged in this search due to the closed hydrogen bond. The input geometries for the keto conformer search were two different enol isomers which are known from their crystal structures and are distinguished by opposite positions of the -OH with respect to the -OMe group on both ends of the molecule.

We found that the keto form bends into many conformations, and we classified those by the degree and angle of bending. We generated several isomers using different random seeds. A conformer search was carried out using a genetic algorithm in Avogadro to obtain a few different keto isomers which were distinguished by the degree of bending.

DFT geometry optimization for all these isomer structures was carried out using the B3LYP functional and the 6-311++G(d,p) basis set, as implemented in the NWChem program.¹⁰ We used the deprotonation site at one of the phenolic -OH form (Figure S3) groups for both the keto-enolic and diketone forms. For the enol form, the deprotonation at the phenolic -OH is

energetically preferred to that at the enolic -OH, as it does not involve the breakage of the intramolecular keto-enolic hydrogen bond.

Electrostatic charges (ESP charges), which are known to yield more accurate CCS values than Mulliken partial charges, for the optimized structures were calculated by fitting to the electrostatic potential calculated using DFT as above with the Merz-Singh-Kollman scheme as implemented in NWChem.¹⁰ These ESP charges were applied for the estimation of theoretical CCSs using the trajectory method (TM) as implemented in the MOBICAL program¹¹⁻¹³ in its modified version for N₂ gas.¹³

The trajectory method (TM) in Mobcal is quite CPU intensive as it runs in serial mode and we restricted its use to only the isomers of curcumin alone, and for the larger curcumin-cyclodextrin complexes we employed the Projection Approximation (PA) method in Mobcal which is known to give accurate values in the size range of molecules of our interest.

A molecular docking¹⁴ study using Autodock 4.2 was applied to build the curcumin \cap CD inclusion complexes.

Computational methods for curcumin-piperine interactions:

Piperine and curcumin have aromatic six-membered rings and hydrogen bond donors and acceptors. Thus they can interact through hydrogen bond and π - π stacking interactions. We have interacted piperine with the each isomer of curcumin through hydrogen bond and π - π stacking interactions. The different possible geometries were optimized using density functional theory calculations. Previous literature showed that Minnesota functionals are suitable for the description of non-covalent interactions.^{15,16} All the geometries were optimized using the M06-2X/6-31G* level of theory. The vibrational analysis revealed that the optimized geometries were corresponding to true minima on the potential energy surface. All the calculations were performed with the help of GAUSSIAN 09 software.

Molecular docking study

We assigned Gasteiger charges to all atoms by following the procedure as implemented in Autodock. For simplicity, we neglected torsional freedom on all molecules which would also result in the glucopyranose units being rotated with respect to each other. The free energies of binding were calculated by summing the intermolecular and internal and torsional terms and

subtracting the unbound energy which is a calculation that is performed within the Autodock program. The size of the search space in which the curcumin isomer (keto/enol) was to be moved was a cube with a side of length of 126 points with point spacing of 0.375 Å. α -CD is the smallest CD consisting of six glucopyranose units and β -CD consists of seven glucopyranose units. The CD molecule consisting of the ring of glucopyranose units has a wide rim known as the head (H) to which the secondary OH groups are bonded and the tail which is a narrower rim to which primary OH groups are added. Head-head orientation in CD dimer was found as the most stable in MD compared to head-tail and tail-tail, as a result of the larger number of intermolecular hydrogen bonds.¹⁷ During the docking simulations, in the monomer complexes, the curcumin isomers (CE1 and CK1) were taken as the “ligand” i.e. the movable molecule whose degrees of freedom would be varied and CDs (α - and β -) as the “receptor” which was the fixed and completely rigid central molecule.

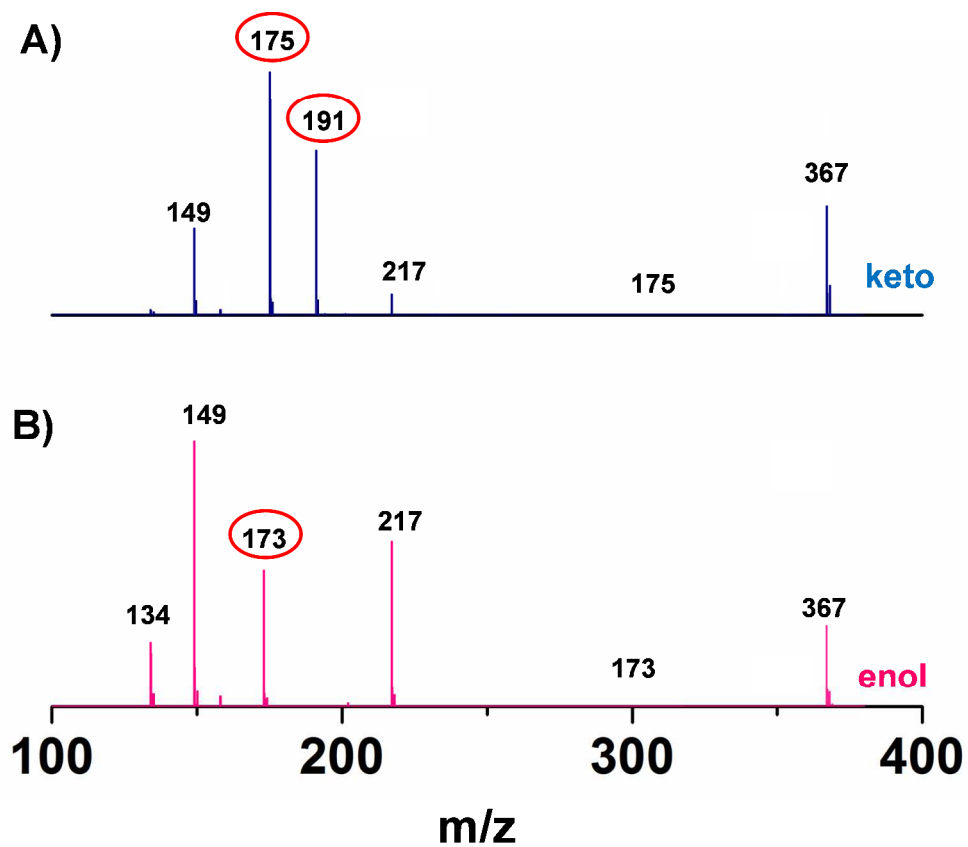


Figure S1. CID mass spectra and fragmentation patterns of isomeric forms of curcumin in transfer CID; **A)** keto form and **B)** enol form. Note the encircled peaks in **A** and in **B**, which are the characteristic fragmentation patterns of keto and enol forms, respectively.

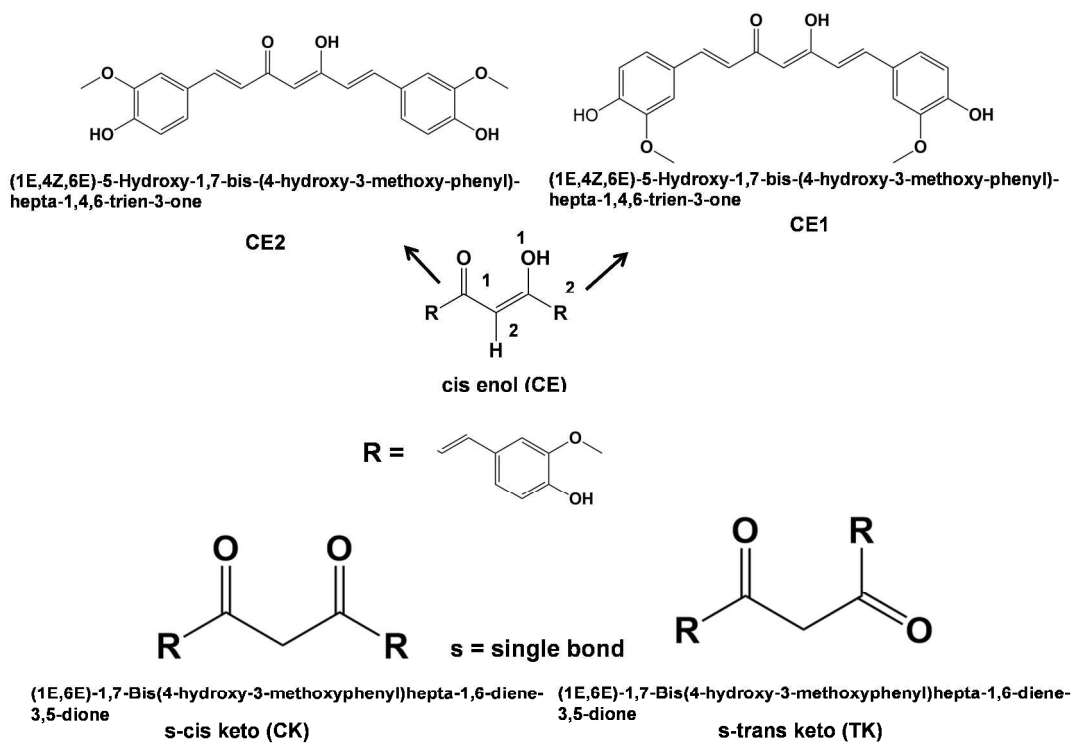
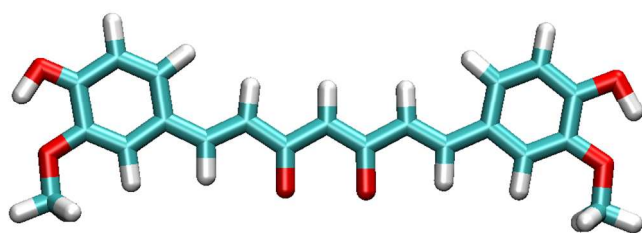


Figure S2. Schematic representation of cis keto-enol forms of curcumin.



EDP (CE2-H)⁻
E = -1263.361 a.u.

Figure S3. DFT optimized EDP (CE2-H)⁻ structure, where EDP stands for enol deprotonation.

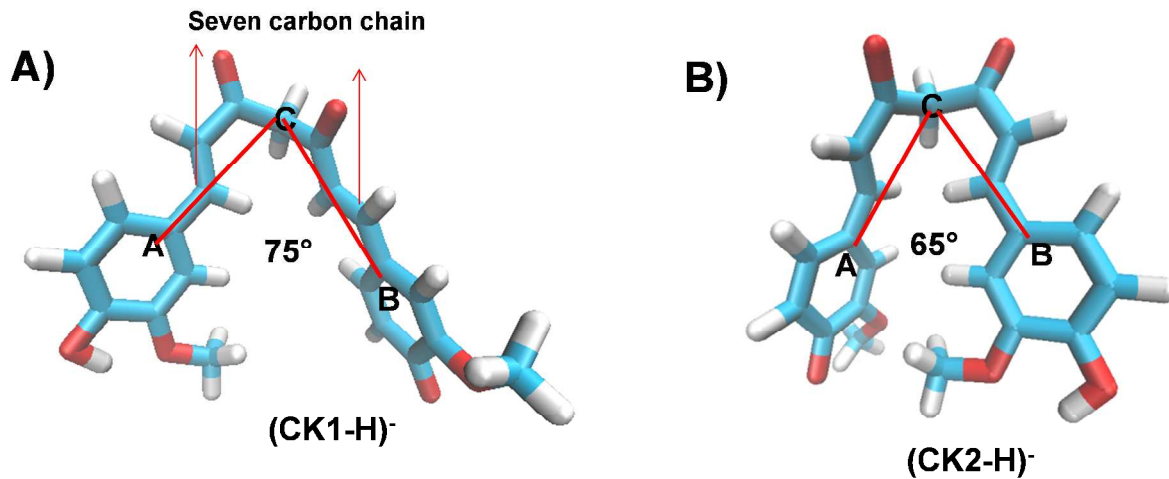


Figure S4. A) & B) Bending angles of (CK1-H)⁻ & (CK2-H)⁻ 75° & 65°, respectively.

Table S1. Experimental and theoretical CCS values

Possible isomers	Energy (in a.u.)	Calculated CCS by TM (Å ²)	Exp. CCS (Å ²)
(CE1-H) ⁻	-1263.389	213.0	
(CE2-H) ⁻	-1263.387	213.5	211.0
(CK1-H) ⁻	-1263.386	198.8	
(CK2-H) ⁻	-1263.382	188.0	196.0

* The isomer labels imply the follows: C, *cis*; E and K, enol and keto.

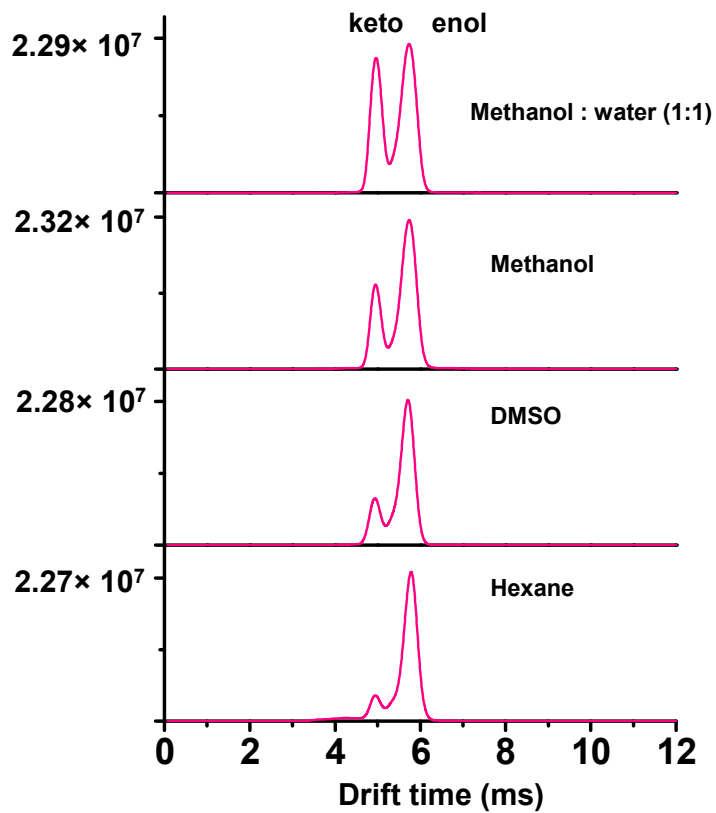


Figure S5. Solvent dependent study of keto-enol isomers. Keeping the concentration of curcumin constant, solvents were changed from non-polar to polar (hexane to methanol/water). With the increase of polarity, the keto form is enhanced.

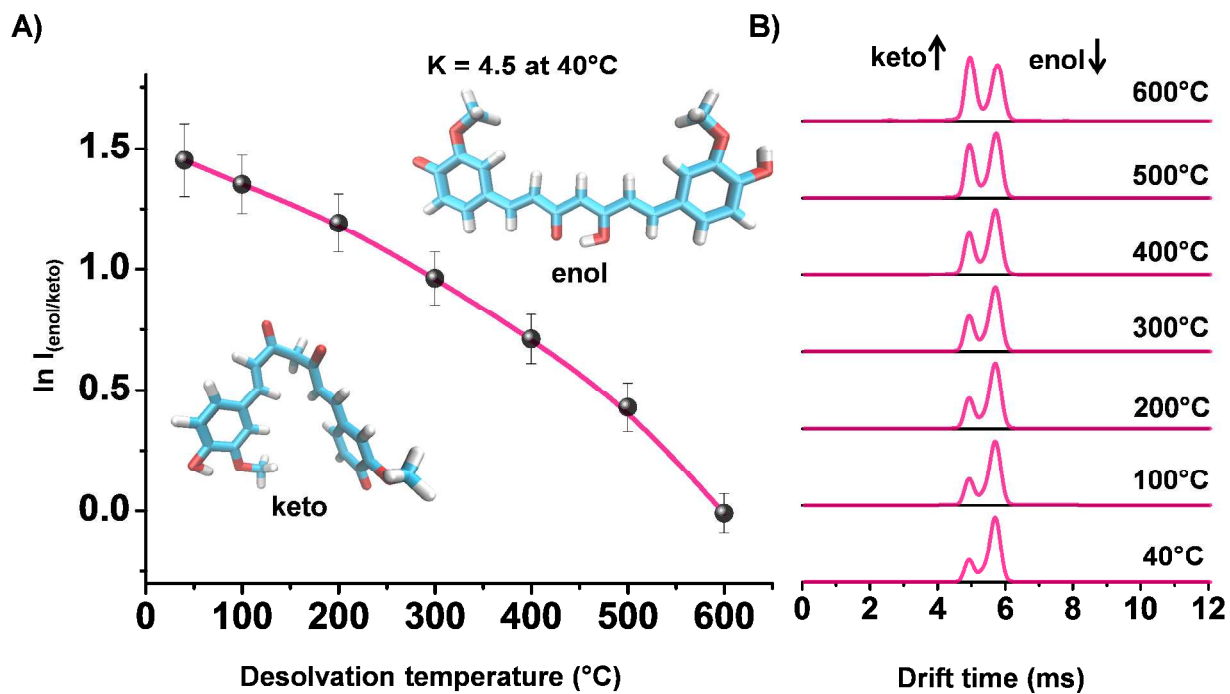


Figure S6. A) Plot of the natural logarithm of keto/enol peak intensity ratios against different desolvation temperatures from 40 to 600 °C. B) With the increase of desolvation temperature, the keto form is enhanced. The lowest energy enol and keto structures are also shown in A).

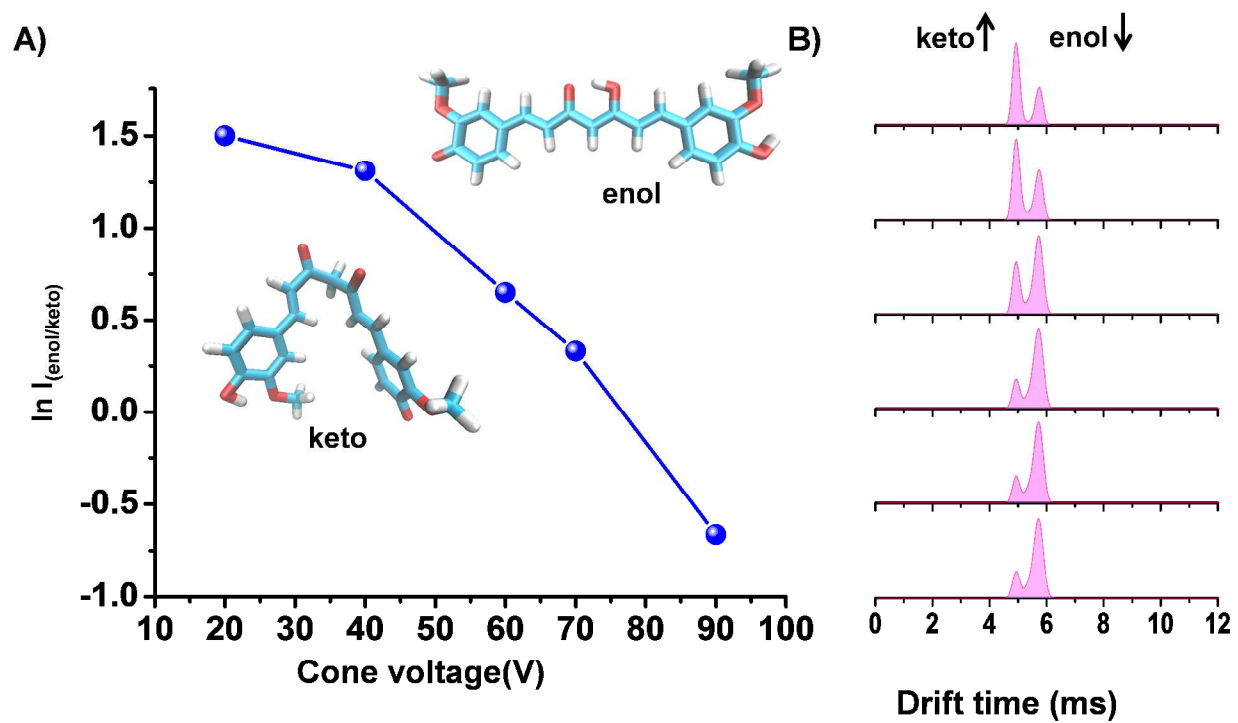


Figure S7. **A)** Plot of the natural logarithm of keto/enol peak intensity ratios against the different cone voltages, from 15 V to 90 V. **B)** With the increase in cone voltage, the enol form decreases.

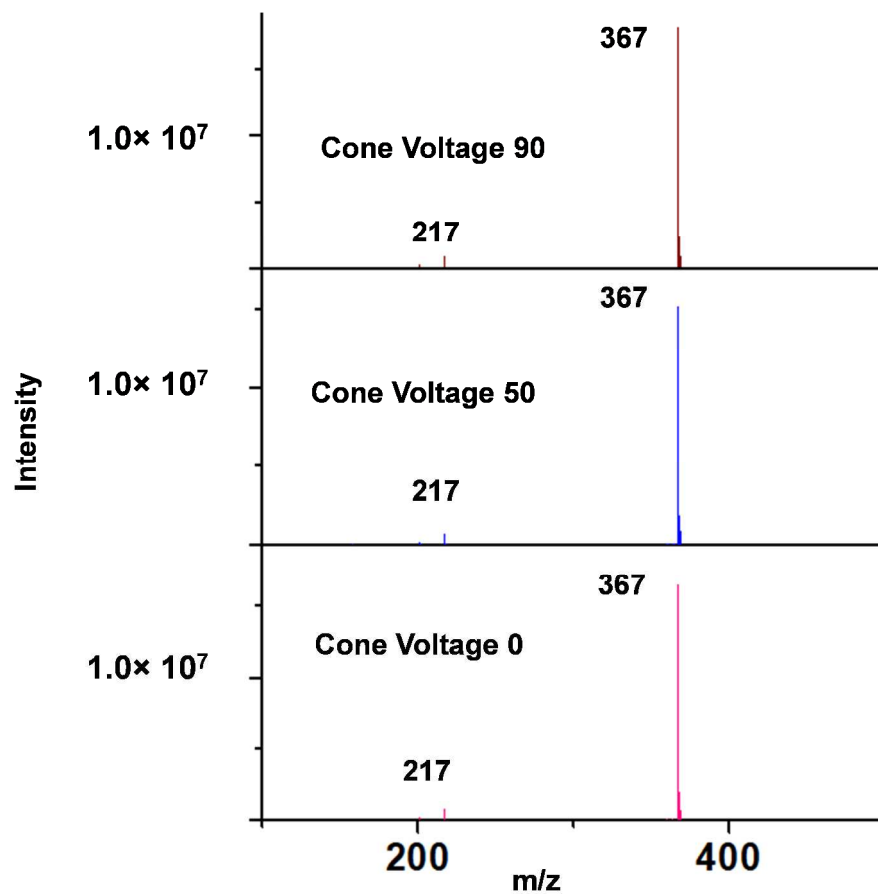


Figure S8. Cone voltage-dependent fragmentation study. No additional change in fragmentation was seen with the increase of cone voltage.

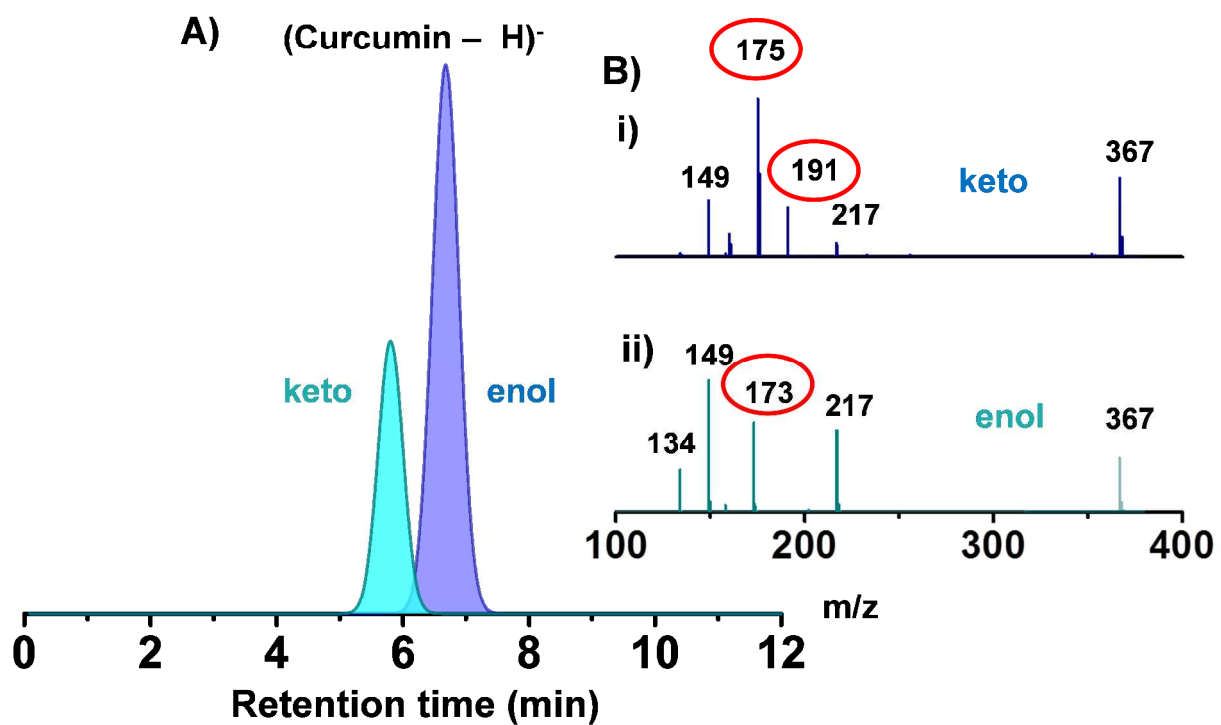


Figure S9. **A)** UPLC separated keto enol tautomers of curcumin. **B)** The MSMS fragmentation of the keto (**i**) and enol (**ii**) forms of curcumin. Tautomer specific peaks are encircled.

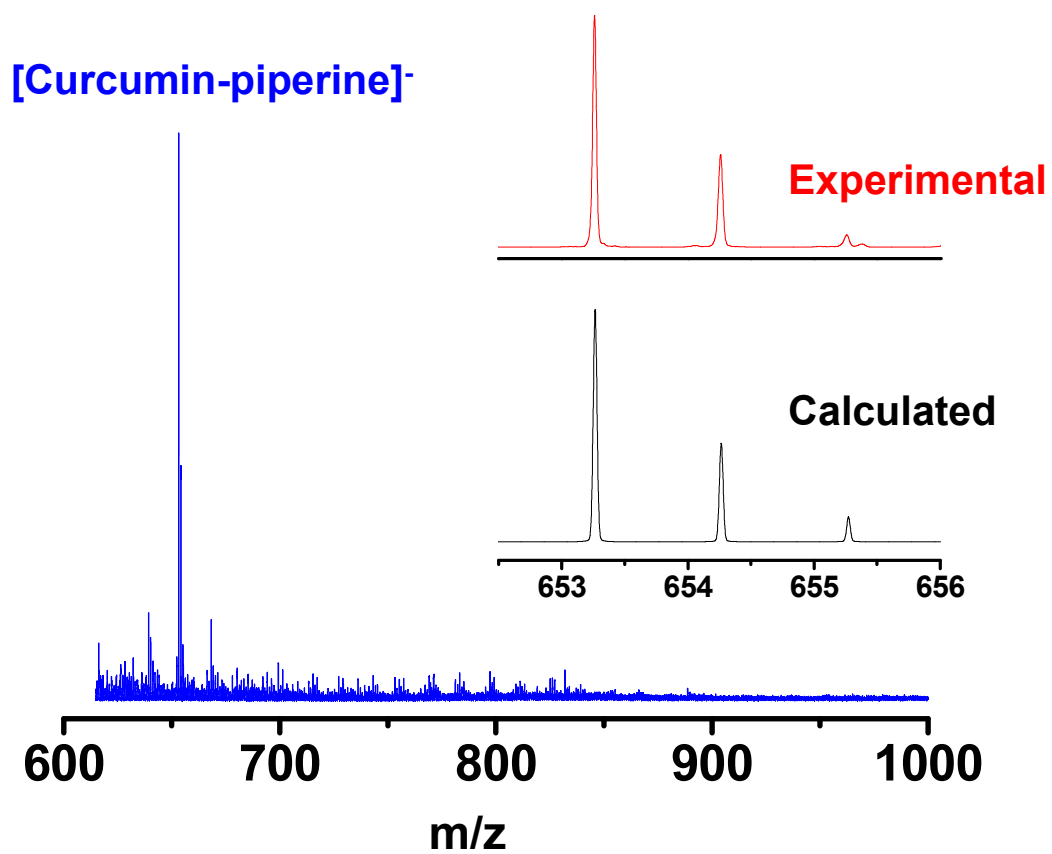


Figure S10. ESI MS of supramolecular adducts of curcumin-piperine complex in ethanol. Inset of the mass spectrum showing that the peak intensities of the isotopologues of the calculated and experimental are matching.

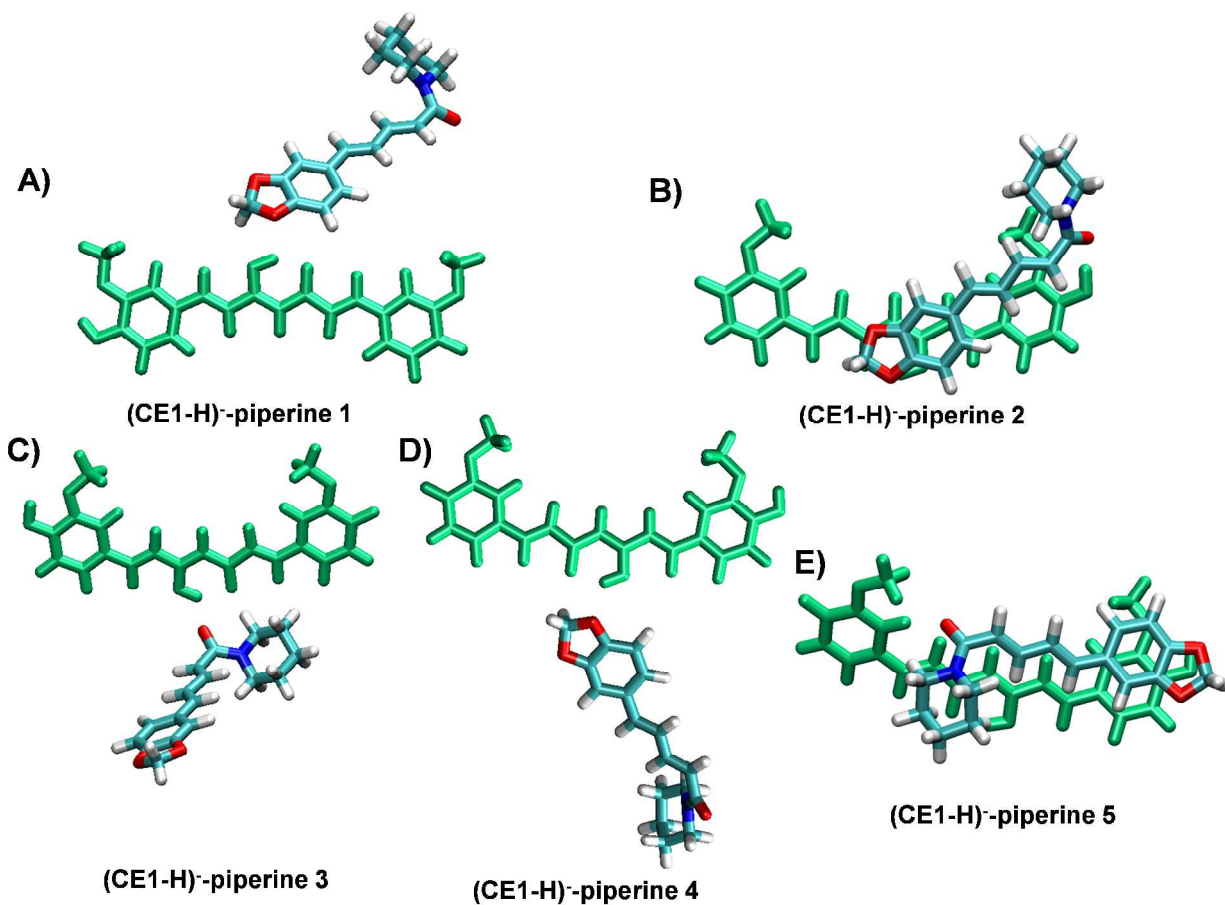


Figure S11. DFT optimized structures of deprotonated (CE1-H)^{•+}-piperine interactions. Different possibilities of structural combination between deprotonated (CE1-H)^{•+} and piperine are shown in A)-E). Among all E) is the lowest energy structure.

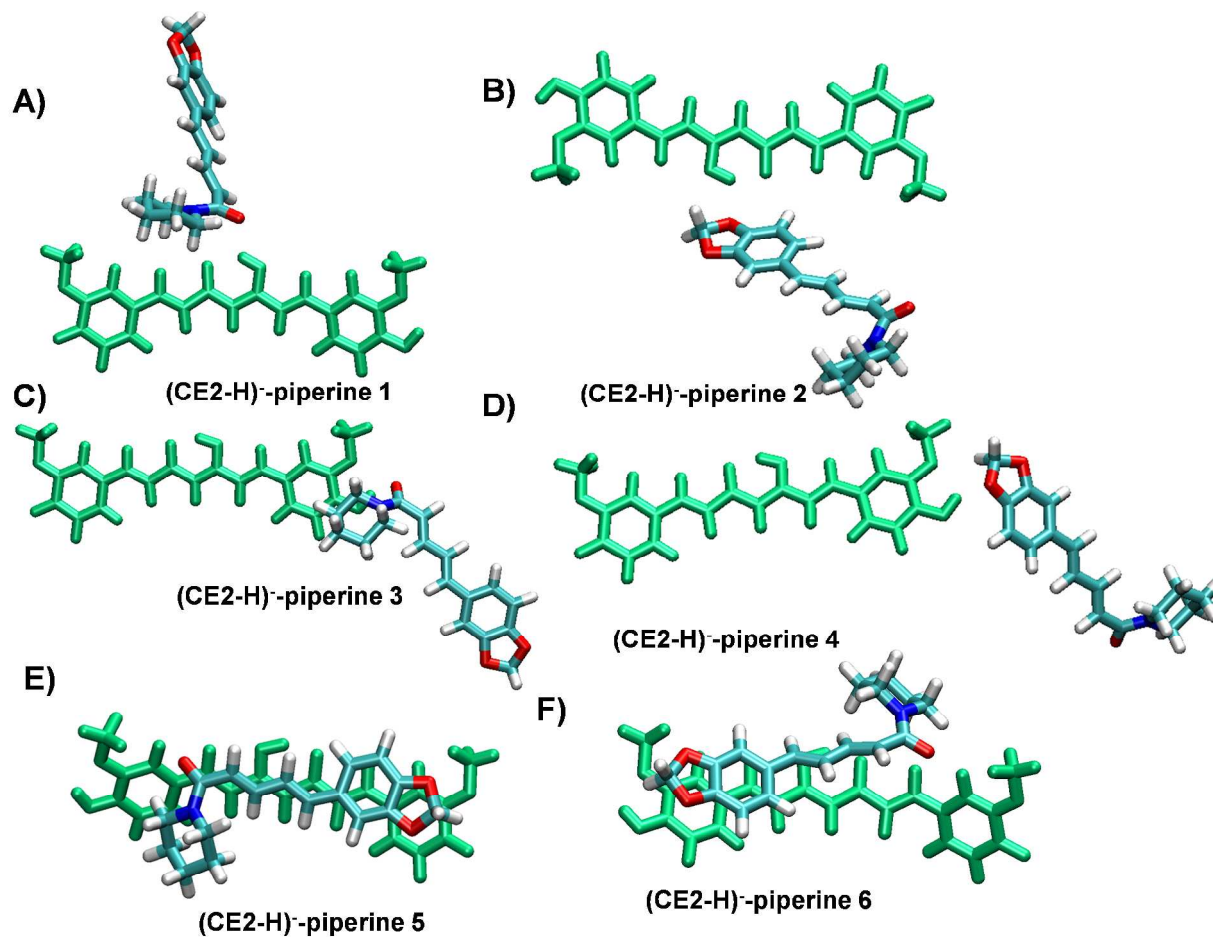


Figure S12. DFT optimized structures of deprotonated (CE2-H)⁻-piperine interactions. Different possibilities of structural combination between deprotonated (CE2-H)⁻ and piperine are shown in A)-F). Among all E) is the lowest energy structure.

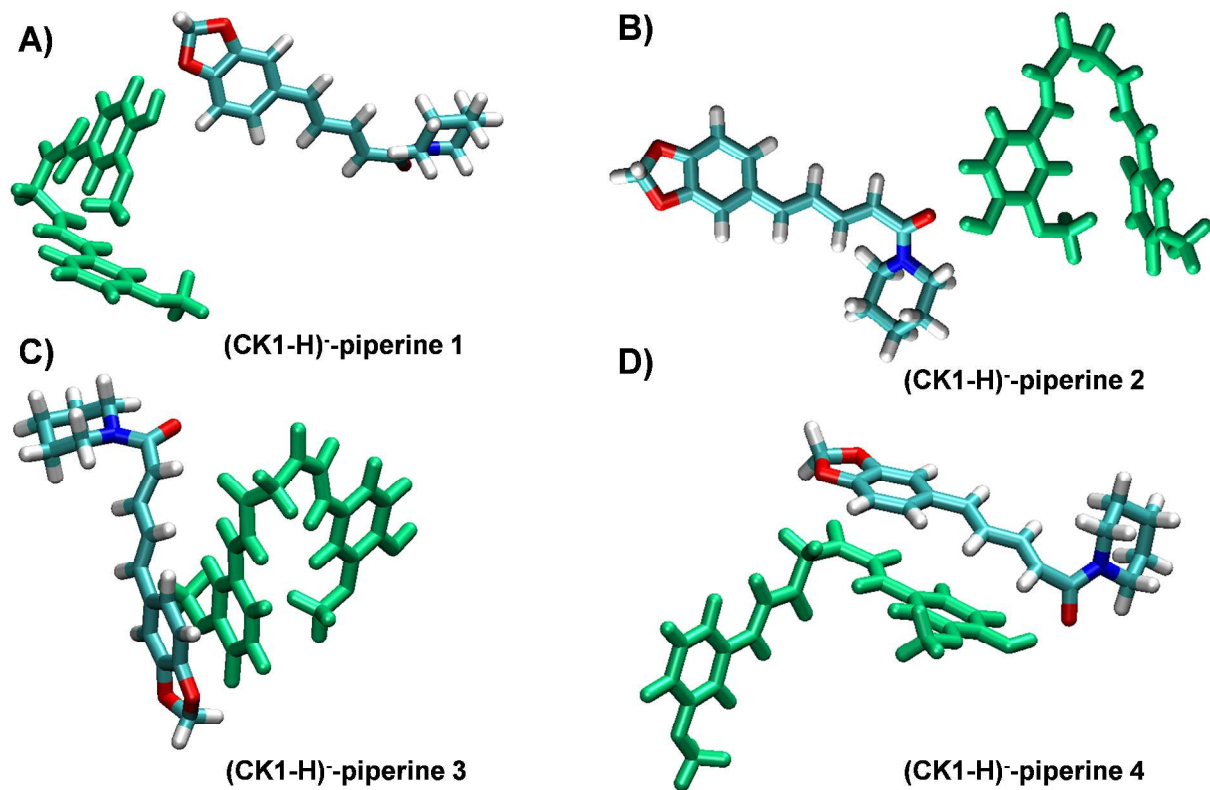


Figure S13. DFT optimized structures of deprotonated (CK1-H)⁻-piperine interactions. Different possibilities of structural combination between deprotonated (CK1-H)⁻ and piperine are shown in A)-D). Among all D) is the lowest energy structure.

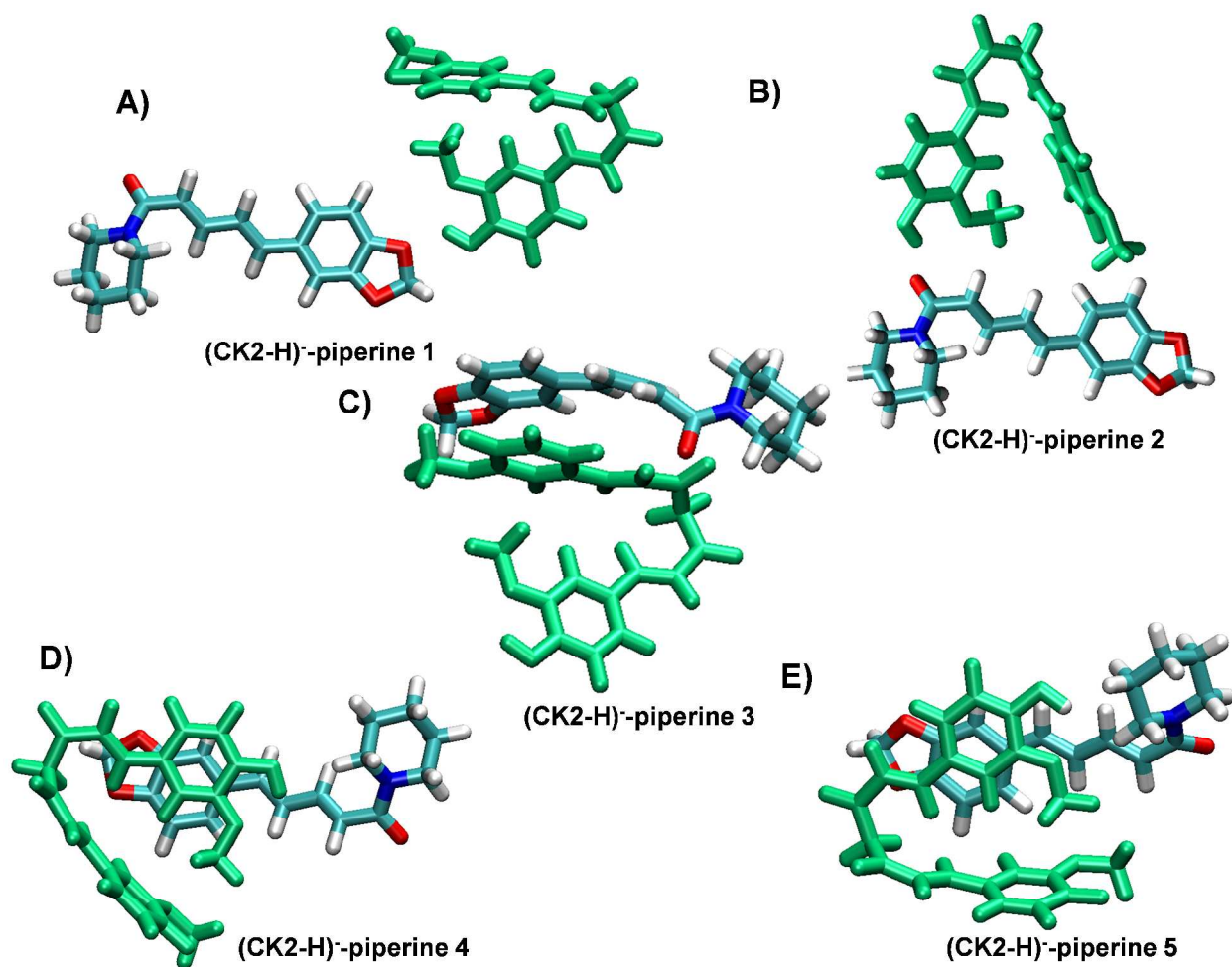


Figure S14. DFT optimized structures of deprotonated (CK2-H)⁻-piperine interactions. Different possibilities of structural combination between deprotonated (CK2-H)⁻ and piperine are shown in A)-E). Among all E) is the lowest energy structure.

Table S2. Relative energies of the (curcumin H)⁻-piperine complexes.

Deprotonated forms of curcumin	Different conformers of curcumin-piperine complexes	Relative energy (kcal/mol)
(CE1-H) ⁻	(CE1-H) ⁻ -piperine 1	20.99
(CE1-H) ⁻	(CE1-H) ⁻ -piperine 2	2.77
(CE1-H) ⁻	(CE1-H) ⁻ -piperine 3	0.69
(CE1-H) ⁻	(CE1-H) ⁻ -piperine 4	20.99
(CE1-H) ⁻	(CE1-H) ⁻ -piperine 5	0.00
(CE2-H) ⁻	(CE2-H) ⁻ -piperine 1	17.76
(CE2-H) ⁻	(CE2-H) ⁻ -piperine 2	18.91
(CE2-H) ⁻	(CE2-H) ⁻ -piperine 3	12.68
(CE2-H) ⁻	(CE2-H) ⁻ -piperine 4	17.30
(CE2-H) ⁻	(CE2-H) ⁻ -piperine 5	0.00
(CE2-H) ⁻	(CE2-H) ⁻ -piperine 6	3.23
(CK1-H) ⁻	(CK1-H) ⁻ -piperine 1	15.22
(CK1-H) ⁻	(CK1-H) ⁻ -piperine 2	8.76
(CK1-H) ⁻	(CK1-H) ⁻ -piperine 3	10.83
(CK1-H) ⁻	(CK1-H) ⁻ -piperine 4	0.00
(CK2-H) ⁻	(CK2-H) ⁻ -piperine 1	14.76
(CK2-H) ⁻	(CK2-H) ⁻ -piperine 2	8.07
(CK2-H) ⁻	(CK2-H) ⁻ -piperine 3	3.46
(CK2-H) ⁻	(CK2-H) ⁻ -piperine 4	3.23
(CK2-H) ⁻	(CK2-H) ⁻ -piperine 5	0.00

Table S3. Most stable curcumin (without proton loss)-piperine complexes with their interaction energies.

Curcumin-piperine complexes	Interaction energy (kcal/mol)
CE1-piperine 5	-23.74
CE2-piperine 5	-21.95
CK1-piperine 4	-22.43
CK2-piperine 5	-18.10

Table S4. Most stable curcumin deprotonated-piperine complexes with their interaction energies.

(Curcumin-H) ⁻ -piperine complexes	Interaction energy (kcal/mol)
(CE1-H) ⁻ -piperine 5	-23.51
(CE2-H) ⁻ -piperine 5	-20.60
(CK1-H) ⁻ -piperine 4	-23.08
(CK2-H) ⁻ -piperine 5	-22.18

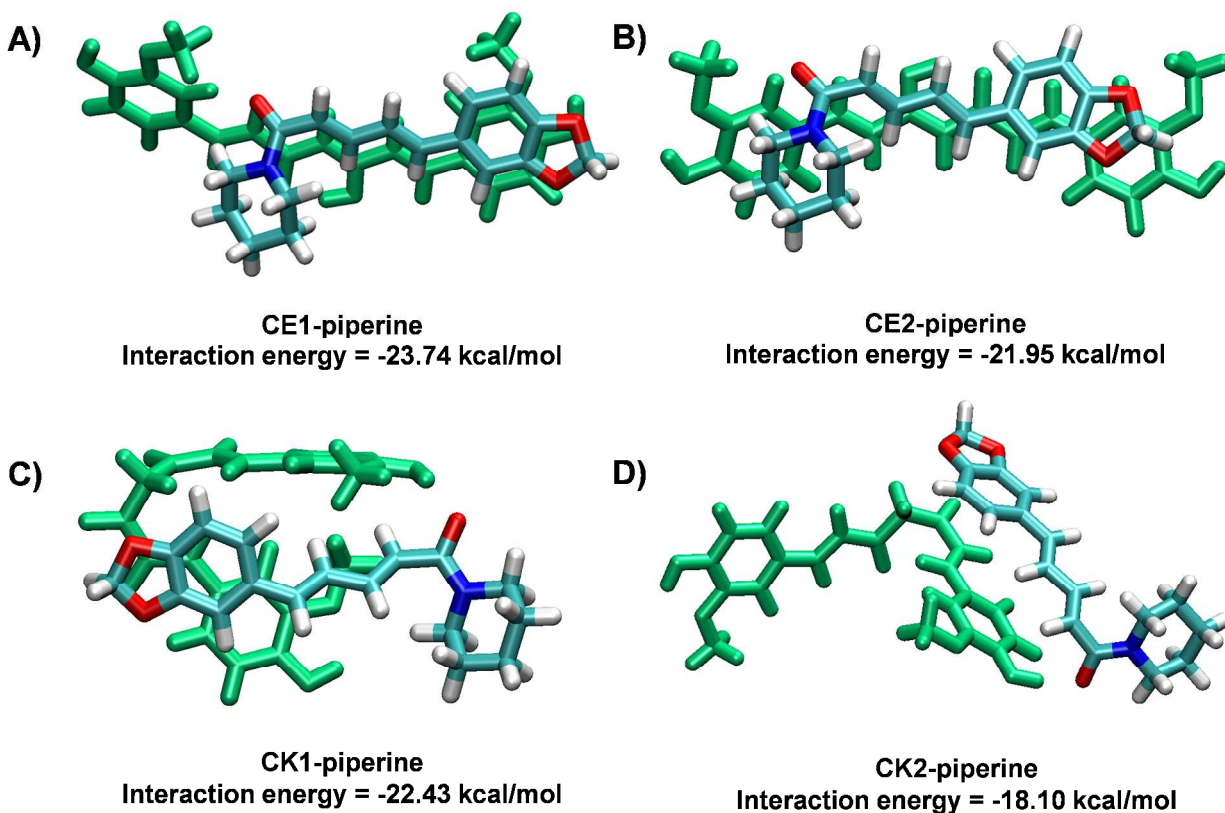


Figure S15. DFT optimized lowest energy structures of A) CE1-piperine, B) CE2-piperine, C) CK1-piperine and D) CK2-piperine, respectively.

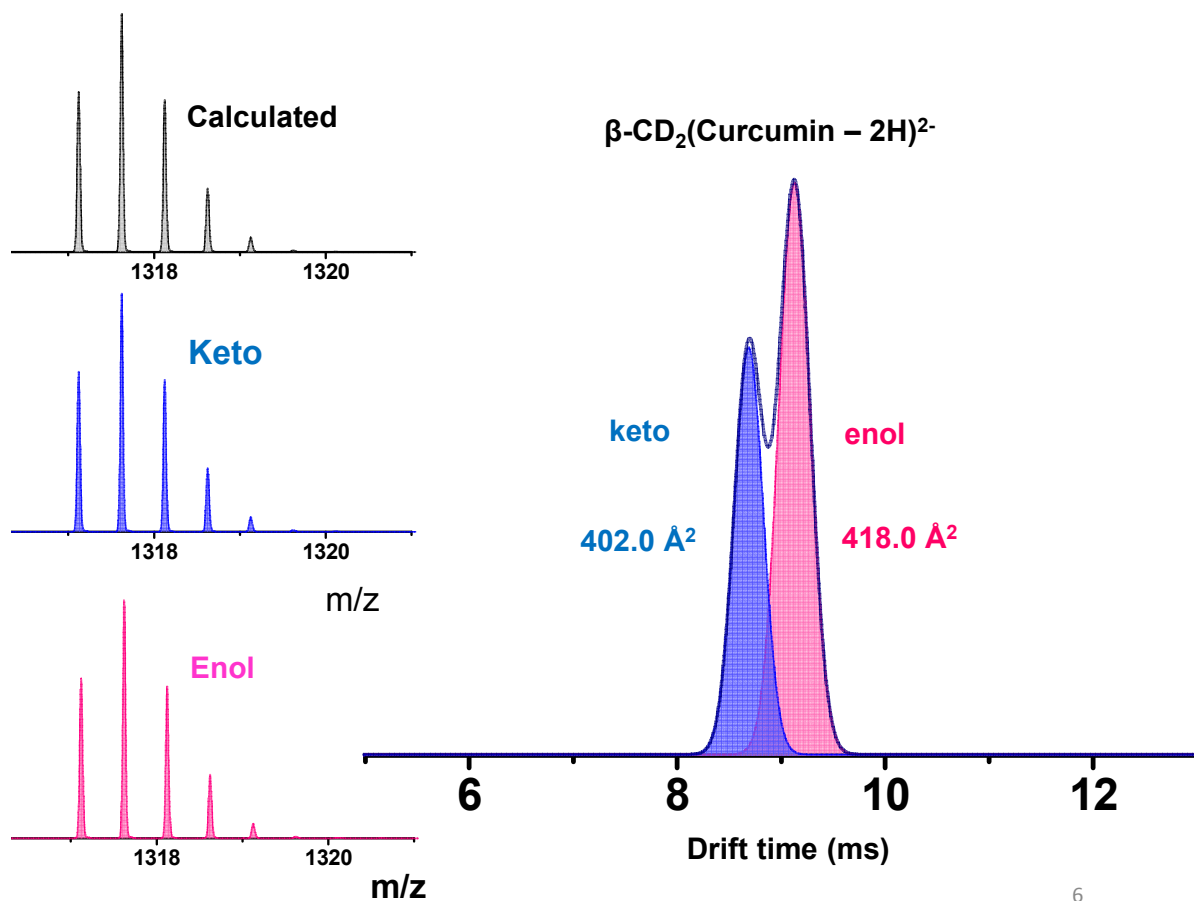


Figure S16. Drift time profile of curcumin- β -cyclodextrin (1:2) inclusion complex; two peaks are indicating the isomeric structures. Inset of drift time profile represents the relative peak intensities of isotopologues of keto and enol inclusion complexes of curcumin which are matching with the calculated peak intensities of the isotopologues.

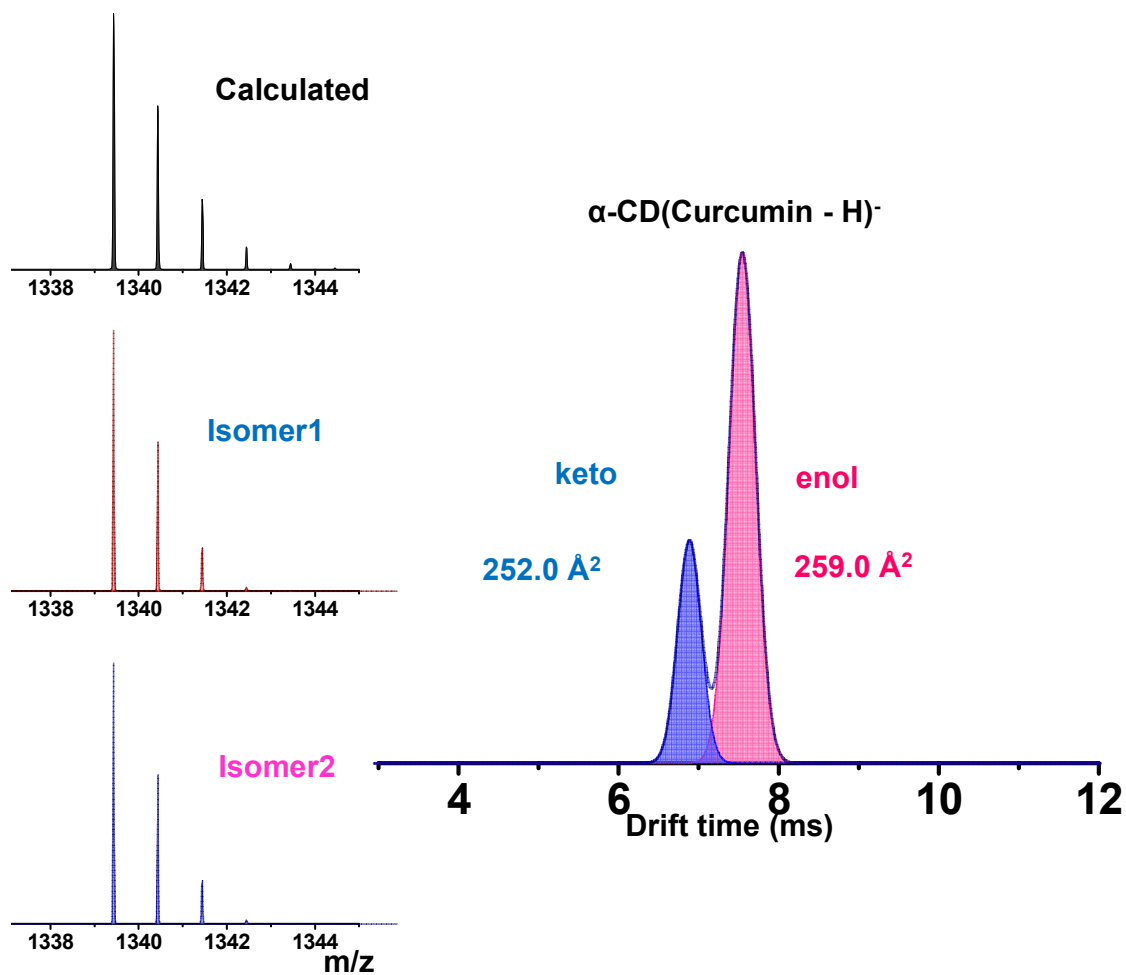


Figure S17. Drift time profile of curcumin- α -cyclodextrin (1:1) inclusion complex; two peaks are indicating the isomeric structures. Inset of drift time profile represents the relative peak intensities of isotopologues of keto and enol inclusion complexes of curcumin which are matching with the calculated peak intensities of the isotopologues.

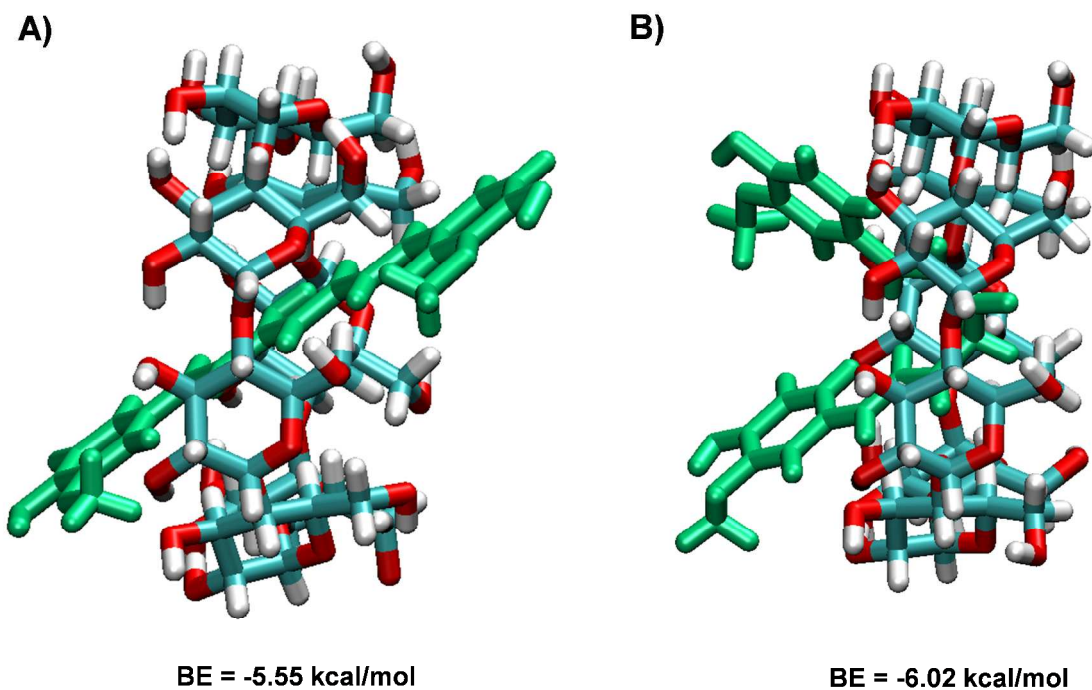


Figure S18. A) & B) CE1 and CK1 docked β -cyclodextrin structures, respectively with binding energies.

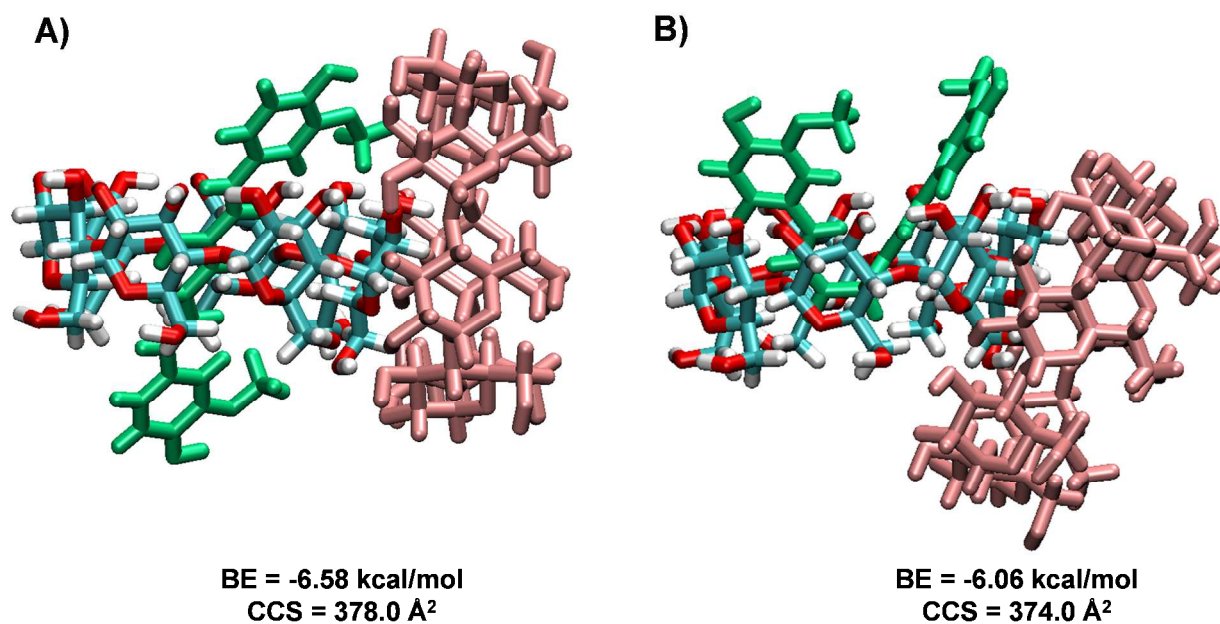


Figure S19. A) & B) Docking of β -cyclodextrin-CE1 and β -cyclodextrin-CK1, respectively with second β -cyclodextrin. Binding energies and CCS values are given below the structures.

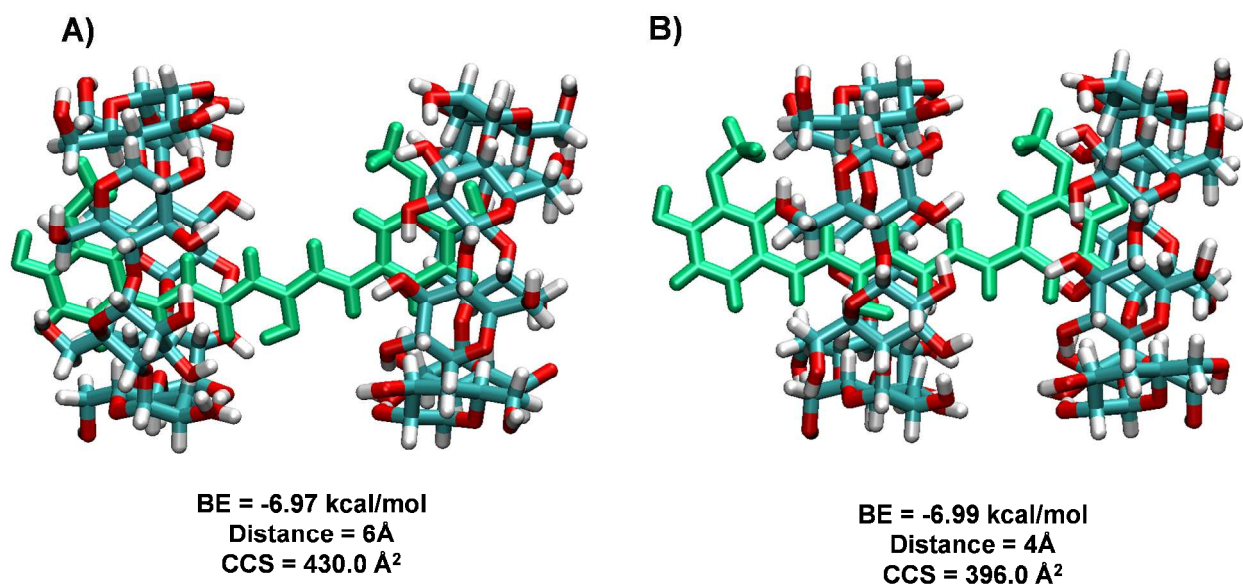


Figure S20. CE1 docked β -cyclodextrin dimer structures. **A)** & **B)** The two β -cyclodextrin dimers were kept apart at 6 Å and 4 Å, respectively. The binding energies, distances and CCS values are provided below each structure.

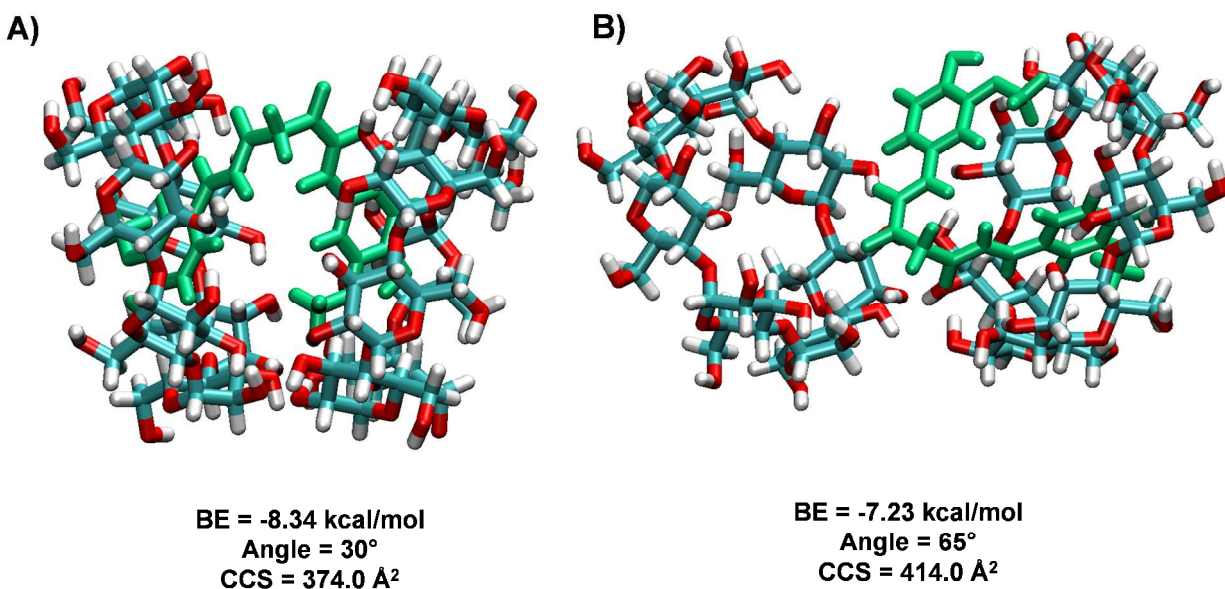


Figure S21. CK1 docked β -cyclodextrin dimer structure. **A)** and **B)** The two β -cyclodextrin dimers were kept apart at different angles 30° and 65°, respectively. The binding energies, angles between the two cyclodextrin and CCS values are given below each structure.

Table S5. CE1-docked β -cyclodextrin dimers with binding energies and CCS values, which are shown for different separation distances of the CD dimers.

Distance between two β -cyclodextrins (\AA^2)	Binding energy of lowest energy conformer (kcal/mol)	Calculated CCS value of lowest energy conformer (\AA^2)	Exp. CCS values (\AA^2)
4	-6.99	396.0	418.0
5	-7.01	411.0	
6	-6.97	430.0	

Table S6. CK1 docked β -cyclodextrin dimer with binding energy and CCS values.

Angle between two β -cyclodextrins	Binding energy of lowest energy conformer (kcal/mol)	Calculated CCS value of lowest energy conformer (\AA^2)	Exp. CCS values (\AA^2)
30°	-8.34	374.0	402.0
40°	-8.58	390.0	
65°	-7.23	414.0	

References

- (1) Forsythe, J. G.; Petrov, A. S.; Walker, C. A.; Allen, S. J.; Pellissier, J. S.; Bush, M. F.; Hud, N. V.; Fernandez, F. M. *Analyst* **2015**, *140*, 6853-6861.
- (2) Slabber, C. A.; Grimmer, C. D.; Robinson, R. S. *J. Nat. Prod.* **2016**, *79*, 2726-2730.
- (3) Renuga Parameswari, A.; Devipriya, B.; Jenniefer, S. J.; Thomas Muthiah, P.; Kumaradhas, P. *J. Chem. Crystallogr.* **2012**, *42*, 227-231.
- (4) Sanphui, P.; Goud, N. R.; Khandavilli, U. B. R.; Nangia, A. *Cryst. Growth Des.* **2011**, *11*, 4135-4145.
- (5) Sanphui, P.; Goud, N. R.; Khandavilli, U. B. R.; Bhanoth, S.; Nangia, A. *Chem. Commun.* **2011**, *47*, 5013-5015.
- (6) Hanwell, M. D.; Curtis, D. E.; Lonie, D. C.; Vandermeersch, T.; Zurek, E.; Hutchison, G. R. *J. Cheminform.* **2012**, *4*, 17.
- (7) Humphrey, W.; Dalke, A.; Schulten, K. *J. Mol. Graphics* **1996**, *14*, 33-38.

- (8) Puliti, R.; Mattia, C. A.; Paduano, L. *Carbohydr. Res.* **1998**, *310*, 1-8.
- (9) Aree, T.; Chaichit, N. *Carbohydr. Res.* **2002**, *337*, 2487-2494.
- (10) Valiev, M.; Bylaska, E. J.; Govind, N.; Kowalski, K.; Straatsma, T. P.; Van Dam, H. J. J.; Wang, D.; Nieplocha, J.; Apra, E.; Windus, T. L.; de Jong, W. A. *Comput. Phys. Commun.* **2010**, *181*, 1477-1489.
- (11) Shvartsburg, A. A.; Mashkevich, S. V.; Baker, E. S.; Smith, R. D. *J. Phys. Chem. A* **2007**, *111*, 2002-2010.
- (12) Mesleh, M. F.; Hunter, J. M.; Shvartsburg, A. A.; Schatz, G. C.; Jarrold, M. F. *J. Phys. Chem.* **1996**, *100*, 16082-16086.
- (13) Siu, C.-K.; Guo, Y.; Saminathan, I. S.; Hopkinson, A. C.; Siu, K. W. M. *J. Phys. Chem. B* **2010**, *114*, 1204-1212.
- (14) Xuan-Yu, M.; Hong-Xing, Z.; Mihaly, M.; Meng, C. *Curr. Comput. Aided Drug Des.* **2011**, *7*, 146-157.
- (15) Mudedla, S. K.; Balamurugan, K.; Subramanian, V. *J. Phys. Chem. C* **2014**, *118*, 16165-16174.
- (16) Mudedla, S. K.; Balamurugan, K.; Kamaraj, M.; Subramanian, V. *Phys. Chem. Chem. Phys.* **2016**, *18*, 295-309.
- (17) Bonnet, P.; Jaime, C.; Morin-Allory, L. *J. Org. Chem.* **2001**, *66*, 689-692.